Contemporary Research Analysis Journal

e-ISSN: 3050-5909
p-ISSN: 3050-5895

Open Access

Volume 03 Issue 11 November 2026
CrossRef DOI: 10.55677/CRAJ/03-2026-Vol03I11

Page no: 864-877

Experimental analysis of Coconut Coir Dust and Acetone Extract as a Low Dosage Hydrate Inhibitor

Adegbaju Oluwaseye Olatunji[1], Uduefe Splendour Esidje[2], Emmanuel Etim Udoessien[3]
[1,2,3]Federal University of Petroleum Resources Effurun

ABSTRACT: Gas hydrates remain one of the most persistent and costly flow assurance challenges in natural gas transportation, and conventional thermodynamic inhibitors such as methanol and monoethylene glycol. This has driven growing interest in low-dosage hydrate inhibitors derived from plant and agricultural waste material, with several recent studies showing such extracts can match or exceed methanol's inhibition performance at a fraction of the dosage. This study investigated coconut dust, a fibrous, lignocellulosic residue from coir processing, as a candidate for this category of inhibitor, a material known to be characterized. Coconut dust extract was obtained from Soxhlet extraction using three solvent systems of increasing polarity, 100% acetone, 50% acetone/50% water, and 70% acetone/30% water, and the resulting extracts were characterized using Fourier Transform Infrared (FTIR) spectroscopy and Thermogravimetric Analysis. Extraction yield was highest for the 50/50 acetone-water system (2.17%), while hydroxyl and phenolic functional-group content, evidenced by FTIR absorption strength, increased consistently with solvent polarity, peaking in the 70/30 acetone-water extract. Thermal analysis showed all three extracts remained stable well beyond typical pipeline operating temperatures, with the pure-acetone extract showing the highest overall thermal robustness and the water-containing extracts decomposing more rapidly and completely. These findings indicate that coconut dust extract, carries phytochemical and thermal characteristics consistent with those associated with effective plant-based hydrate inhibitors

KEYWORDS: Coconut dust extract, low dosage hydrate inhibitor, gas hydrate, Soxhlet extraction, FTIR, thermogravimetric analysis.

Cite the Article: *Olatunji, A.O., Esidje, U.S., Udoessien, E.E. (2026). Experimental analysis of Coconut Coir Dust and Acetone Extract as a Low Dosage Hydrate Inhibitor. Contemporary Research Analysis Journal, 3(11), 864-877.https://doi.org/10.55677/CRAJ/03-2026-Vol03I11*

License: This is an open-access article under the CC BY 4.0 license: https://creativecommons.org/licenses/by/4.0/

Publication Date: November 13, 2026

**Corresponding Author: Uduefe Splendour Esidje*

INTRODUCTION

1.1 Background to the study

Natural gas rarely makes the journey from reservoir to end user without a fight along the way. Somewhere between the wellhead and the processing plant — inside a subsea flowline, a gathering pipeline, or a compressor station the gas encounters water it has not fully shed, and if the pressure climbs high enough while the temperature drops low enough, the two combine into something the industry has learned to dread: gas hydrates. These are icelike crystalline solids in which water molecules arrange themselves into cage-like lattices around individual gas molecules such as methane, ethane, or carbon dioxide (Almashwali et al., 2022). They are not chemical compounds in the conventional sense, since no covalent bond forms between the host water and the trapped gas; the cage simply holds the guest molecule in place physically. But the practical result is every bit as troublesome as a true solid deposit, because once nucleation begins, hydrate crystals grow, clump together, and eventually accumulate into plugs capable of shutting an entire line.

The problem has a long history. It was first documented in 1934, when Hammerschmidt traced a string of pipeline blockages in American gas transmission systems to hydrate formation rather than to ice, as had been widely assumed until then (Almashwali et al., 2022). That single observation reshaped how the industry thought about pipeline design and operation, because it revealed that hydrates could form at temperatures well above the freezing point of water, provided the pressure was high enough conditions that are, unfortunately, completely ordinary in deep-water and cold-climate gas operations. Nearly a century later, hydrate control remains one of the central concerns of flow assurance, the branch of petroleum engineering dedicated to keeping hydrocarbons moving reliably and safely from reservoir to delivery point.

The cost of getting it wrong is not abstract. A hydrate plug in a subsea flowline can take days or weeks to clear, depending on its size and location, and the remediation options- depressurising the line, applying external heat, injecting methanol directly at the blockage, or, in the worst cases, mechanically intervening are all expensive, timeconsuming, and carry their own safety risks. Beyond the direct cost of the shutdown, there is lost production, potential equipment damage from the pressure differentials involved in clearing a plug, and, in offshore settings, genuine risk to personnel. It is this combination of frequency, cost, and hazard that has kept hydrate inhibition research active and well-funded for decades.

The default weapon against hydrate formation has been the thermodynamic inhibitor, chiefly methanol and monoethylene glycol (MEG). These work by shifting the pressure–temperature equilibrium curve at which hydrates form, effectively pushing the hydrate stability region toward lower temperatures and higher pressures than the system will normally encounter. The chemistry is straightforward and well understood, and both chemicals have been proven in the field for generations. Though their effectiveness comes at a structural cost: because they work thermodynamically rather than kinetically, they need to be present in large quantities relative to the water in the system, typically somewhere between 10% and 60% of the water volume, depending on the severity of the subcooling involved. On a long subsea tie-back or in a high-water-cut field, that translates into enormous volumes of chemical that must be purchased, transported, stored, and often regenerated to keep the operation economical.

The environmental side of the ledger is no kinder. Methanol is volatile, flammable, and toxic enough that its presence in produced water discharged into marine environments is a genuine regulatory and ecological concern. MEG is less acutely toxic but is considerably more expensive and requires a dedicated recovery and regeneration unit to be viable at scale, adding capital cost to every project that relies on it. Neither chemical, in short, is a solution anyone is entirely comfortable with; they are simply the tools that have worked reliably enough, for long enough, to remain the industry default.

This tension between reliability and cost is what drove the development of low dosage hydrate inhibitors (LDHIs) beginning in the early 1990s. Unlike thermodynamic inhibitors, LDHIs do not attempt to move the equilibrium curve at all. Instead, they intervene in the kinetics of hydrate formation. Kinetic hydrate inhibitors (KHIs) are typically water-soluble polymers that adsorb onto the surface of forming hydrate crystals and physically interfere with further growth, buying enough time- often several hours for the fluid to clear the hydrate-risk zone of the pipeline before a stable crystal structure can form (Kelland et al., 2024). Anti-agglomerants (AAs), the other major class of LDHI, take a different approach: they do not necessarily prevent hydrate crystals from forming at all, but they keep the resulting particles small and dispersed, so that instead of consolidating into a plug, the hydrates simply flow through the pipeline as a transportable slurry. Because both mechanisms act on the surface chemistry of the hydrate rather than on the bulk thermodynamics of the system, LDHIs are typically effective at concentrations of less than 1% by volume of water a fraction of what thermodynamic inhibitors require.

The catch is that most commercial LDHIs are themselves synthetic polymers, such as polyvinylcaprolactam and polyvinylpyrrolidone. They are far more efficient by volume than methanol or MEG, but they are not necessarily biodegradable, and they are not inexpensive to manufacture at industrial scale. This has, over the past decade, opened the door to a growing body of research into plant-derived and agro-waste-derived LDHIs extracts that occur naturally, that in many cases are already treated as waste, and that a cluster of recent Nigerian flow-loop studies have shown to perform surprisingly well against gas hydrates. Elechi et al. (2018, 2021) demonstrated, using a locally fabricated mini flow loop, that plant extracts and locally sourced surfactants could inhibit hydrate formation as effectively as, or in some cases better than, conventional MEG. More recently, Ndoma-egba et al. (2025) tested Moringa oleifera leaf extract against methanol across a range of concentrations and found that just 0.04 wt% of the extract achieved a 60% inhibition efficiency, edging out methanol's best result of 56.7% at 2 wt%- a fiftyfold reduction in the quantity of active material required for a better outcome.

This project situates itself within that same research tradition, but turns attention to a material that has received almost no direct study as a hydrate inhibitor candidate: coconut coir dust, the fine, fibrous residue left over once coconut husks have been processed for coir fibre. Coconut coir dust is agricultural waste in the most literal sense. It is produced in large volumes wherever coconut is processed commercially; it is currently put to little use beyond low-value soil conditioning, and prior characterisation work on related coconut by-products has shown it to be rich in lignin, hemicellulose, tannins, and other phytochemicals several of which are already known, from corrosioninhibition and other green-chemistry literature, to be surface-active or thermally robust compounds. If an extract drawn from this material can be shown to carry the functional-group chemistry and thermal stability associated with effective hydrate inhibition, it represents exactly the kind of cheap, renewable, and biodegradable LDHI candidate the industry has been actively searching for.

1.2 Statement of the Problem

Conventional hydrate inhibitors solve the flow assurance problem but create two new ones: cost and environmental exposure. Methanol and MEG remain the default in many operations not because they are ideal, but because they are proven and readily available, even though their large dosage requirements, aquatic toxicity, and regeneration overheads are well documented (Ndoma-egba et al., 2025). Synthetic LDHIs reduce the dosage problem but do not fully resolve the environmental one, and they remain comparatively costly to produce at scale.

Agro-waste-derived extracts have shown real promise as a third path, but the pool of tested candidates remains small, and almost all existing work has focused on leafy plant material (Moringa, cassava leaves, Terminalia catappa leaves) rather than on lignocellulosic waste products such as coconut dust. Coconut dust's phytochemical and thermal profile has never, to the researcher's knowledge, been evaluated specifically with hydrate inhibition potential in mind. This leaves a gap: a widely available, essentially free agricultural by-product remains uncharacterized for a use that could add genuine value to it, while the industry continues to depend on inhibitors with well-known drawbacks.

1.3 Aim and Objectives of the Study

AIM:

To experimentally Analyze Coconut Coir Dust and Acetone Extract as a Low Dosage Hydrate Inhibitor

The objectives are to:

1. Extract bioactive compounds from coconut dust using a Soxhlet extraction method across three solvent systems of varying polarity (100% acetone, 50% acetone/50% water, and 70% acetone/30% water), while determining the solvent ratio that yields the most promising extract.
2. Characterize the functional group composition of each CCDE extract using Fourier Transform Infrared (FTIR) spectroscopy to identify the presence of hydroxyl, carbonyl, and other functional groups associated with known hydrate-inhibiting phytochemicals.
3. Evaluate the thermal stability and decomposition behavior of each extract using Thermogravimetric Analysis (TGA) and its derivative (DTG) to assess how the material would hold up under pipeline operating conditions.
4. Compare the extraction yield, functional group profile, and thermal behaviour across the three solvent systems to identify the most suitable formulation for future hydrate inhibition testing.
5. Evaluate, based on these findings and comparison with existing literature on plant-based LDHIs, the potential of CCDE as a viable, lower-cost, and more environmentally friendly alternative to conventional inhibitors such as methanol.

LITERATURE REVIEW

2.1 Conceptual Review/Theoretical Framework

2.1.1 Natural Gas Hydrates: Structure and Formation Conditions

Ice that isn't cold- that's the strange fact sitting at the centre of the gas hydrate problem. These crystalline solids can form at 15 to 20°C, comfortably above the freezing point of water, provided the pressure is high enough to make up the difference. A gas hydrate, more precisely a clathrate hydrate, forms when water molecules lock themselves into a cage-like lattice around a smaller guest molecule, usually methane or another light hydrocarbon common in natural gas. No chemical bond forms between the two. The water simply holds the gas in place, physically rather than chemically, so a hydrate can be broken apart just by shifting pressure or temperature, without needing any reaction to undo it.

Three crystal structures show up in the literature — sI, sII, and sH — sorted by cage size. Structure I is the one that matters most for this study's context, since it forms around small molecules like methane and is the structure typically found clogging natural gas transmission pipelines. Structure II needs slightly bigger guests, propane and isobutane, and turns up more often in associated gas systems.

The problem has a fairly precise birthdate in the engineering literature: 1934, when E.G. Hammerschmidt showed that a string of pipeline blockages everyone had blamed on ice were actually gas hydrates. That one correction reshaped how the industry thought about dehydration and pipeline design, because it meant hydrates weren't confined to freezing conditions — they could ambush a line running at a perfectly ordinary temperature, provided the pressure cooperated. Ninety years later, that finding still underpins nearly every hydrate-inhibition study referenced in this chapter.

2.1.2 Flow Assurance and Why Hydrate Control Actually Matters

Flow assurance is the part of the petroleum engineering job that nobody notices when it's working. Its whole purpose is keeping oil and gas moving from reservoir to sales point without interruption no hydrate plugs, no wax, no scale, no sand. Of these, hydrates tend to be the one operators fear most, not because they're mysterious, but because they can form fast (field cases exist of plugs forming within hours of a shut-in) and clearing one is neither quick nor cheap. Depressurizing from both ends, applying heat, injecting chemical directly at the blockage, or in the worst cases physically intervening every option costs money, costs time, and carries some risk of the plug itself becoming a hazard if pressure is released carelessly. That combination of speed, cost, and danger is exactly why decades of research money has gone into finding cheaper, safer ways to keep hydrates from forming in the first place.

2.1.3 Three Ways to Fight a Hydrate

Broadly, the industry has three tools. Thermodynamic hydrate inhibitors methanol and monoethylene glycol (MEG) being the household names work by shifting the pressure-temperature curve at which hydrates become stable, pushing that boundary toward conditions the pipeline won't actually reach. Because this is a bulk, colligative effect, it takes a lot of chemical to pull off: typically 10–60% of the water volume in the system, depending on how far the operating conditions sit inside the hydrate stability zone (a gap engineers call subcooling).

Kinetic hydrate inhibitors (KHIs) take a completely different approach. Rather than moving the equilibrium at all, they interfere with the kinetics (the speed) of crystal growth. These are usually water-soluble polymers that latch onto a forming hydrate crystal's surface and physically get in the way of further growth, buying time for the fluid to clear the danger zone before a solid plug can consolidate. Because they're working at the crystal surface rather than throughout the bulk water, a KHI can do its job at well under 1% of the water volume a fraction of what a thermodynamic inhibitor needs.

Anti-agglomerants (AAs) are the third option, and they don't try to stop hydrate crystals from forming at all. Instead, they keep the crystals small and separated, dispersed through the oil phase as a slurry that can still be pumped rather than left to clump into something solid. KHIs and AAs together get grouped under the umbrella term low dosage hydrate inhibitors (LDHIs) a name that says exactly what matters about them: they work at a fraction of the volume a thermodynamic inhibitor requires.

2.1.4 Why "Green" LDHIs Are Even a Question Worth Asking

Here's the catch with most commercial LDHIs: they're synthetic polymers polyvinyl caprolactam and its relatives and while they're far more dosage-efficient than methanol, they aren't cheap to make and aren't necessarily biodegradable. That gap is what's pulled a fairly young research community, concentrated heavily in Nigerian petroleum engineering departments, toward asking whether extracts from ordinary plants or agricultural waste could do a similar job. The working idea is that certain phytochemicals tannins, saponins, flavonoids, and related polyphenols are polar or amphiphilic enough to interact with a growing hydrate crystal's water lattice in roughly the way a synthetic KHI does.

2.1.5 What Coconut Dust Actually Is

Coconut coir dust is the fine, spongy leftover material once the coarser fibers have been stripped out of coconut husk during coir processing. It's lignocellulosic biomass: mostly cellulose, hemicellulose, and lignin, in proportions that shift depending on the coconut variety and how mature the husk was, but generally lignin-heavy compared to most other agricultural residues. That lignin content is actually why materials scientists and soil scientists have already taken an interest in coir pith for bio composites in the first case, for water retention as a peat substitute in the second. Buried within that fibrous structure are smaller amounts of extractable compounds: tannins, polyphenols, and other secondary metabolites, which is the fraction this study's Soxhlet extraction is actually going after, and the fraction whose chemistry and thermal behavior gets characterized in Chapter Four.

2.1.6 Why Solvent Choice Matters So Much

Extraction works on a fairly simple principle: pick a solvent that dissolves the compound you want more readily than it dissolves everything else in the solid matrix, and the target compound comes out into the liquid while the bulk of the structural material stays behind. Soxhlet extraction, the method used here and described in full in Chapter Three, does this through repeated cycles the solvent evaporates, condenses, and percolates back through the sample over and over, so fresh solvent keeps contacting the material until there's nothing left worth pulling out.

The single biggest lever in this process is solvent polarity. Non-polar solvents like hexane go after lipids and waxes; polar solvents like water and methanol go after phenolics and tannins. Acetone sits in the middle, which is exactly why it gets blended with water at different ratios to dial polarity up or down the same logic behind this project's three solvent systems (100% acetone, 50/50 acetone-water, and 70/30 acetone-water).

2.1.7 Reading a Molecule's Fingerprint with FTIR

FTIR spectroscopy works by finding out which infrared wavelengths a sample absorbs, since every type of chemical bond — O–H, C=O, C–H, C–O, aromatic C=C — vibrates at its own well-documented frequency. It won't tell you exactly which compound you're looking at (that job belongs to something like GC-MS), but for a crude extract, it's more than enough to confirm which broad functional-group families are present. A broad O–H stretch somewhere around 3200–3550 cm^{-1} points to hydroxyl-rich phenolics. A C=O stretch near 1700–1750 cm^{-1} suggests tannins or carboxylic acids. A C=C stretch around 1600–1620 cm^{-1} is consistent with the aromatic rings found in flavonoids.

That's the lens this study uses to read the CCDE spectra in Chapter Four.

2.1.8 What TGA Actually Shows

Thermogravimetric analysis heats a sample on a controlled ramp usually room temperature up to 900–950°C and tracks how much mass it loses along the way. For something like a lignocellulosic extract, the pattern is fairly predictable: a small early loss below about 150°C from residual moisture, then the big event, usually somewhere between 200°C and 400°C, where hemicellulose and other less-stable organics break down, then a long, slow tail out to high temperature as lignin decomposes. Take the derivative of that curve (DTG), and the transitions sharpen into clear peaks, making it easy to pin down exactly where decomposition is happening fastest. Why does this matter for hydrate inhibition specifically? Because any real candidate inhibitor needs to survive the temperatures it would actually meet in a pipeline (not an extreme bar), since pipelines rarely run past 100°C, but one worth confirming with data instead of just assuming.

2.2 Empirical and Experimental Literature Review

2.2.1 Gas Hydrate Fundamentals and Flow Assurance

Starting with Englezos's review of clathrate hydrate crystallization in the Canadian Journal of Chemical Engineering, it works through classical nucleation theory as applied to hydrates, spends real time on induction time that delay between hitting hydrate-

favorable conditions and actually seeing the first crystal and ties all of it back to gas processing and transport concerns. For this project, the value is foundational rather than direct: induction time is exactly what kinetic inhibitors are built to stretch out, so understanding it is a prerequisite for even asking whether a compound's functional-group chemistry might matter to hydrate nucleation. What it doesn't do, and this will become a running theme is say a single word about plant-derived or agro-waste inhibitors. That's not a criticism so much as a reflection of when it was written, well before green LDHIs became a research interest.
In the Transactions of the Indian Institute of Metals covers similar ground from a slightly different angle, tracing hydrate science back to Humphry Davy's 1811 discovery of chlorine hydrate and forward to modern spectroscopic studies of cage occupancy. Its usefulness here is in the phase-boundary detail understanding how gas composition shifts the pressure-temperature curve is necessary background for making sense of the flow-loop conditions. Same gap as Englezos, though: no bio-based inhibitors anywhere in it.
Almashwali et al. (2022), in ACS Omega, narrows the focus to oil-dominant multiphase systems which matters more for this project's context than it might first sound, since Niger Delta pipelines typically carry oil-dominant rather than pure dry-gas streams. What makes this one genuinely useful is its tabulation of experimental hydrate studies by inhibitor type and test condition. It also lays out anti-agglomerant mechanisms clearly, filling a gap Englezos leaves in the kinetic-inhibitor-heavy older literature. But the inhibitor coverage stops at synthetic anti-agglomerants, KHIs, and THIs, plant extracts don't make an appearance, which says something about how recent and geographically concentrated that specific research thread still is.
A broader review on flow assurance issues in gas pipeline transmission takes a step back and places hydrates alongside wax, scale, corrosion, and asphaltenes: arguing, reasonably, that you can't really solve hydrate control in isolation from these other problems, since fixing one (say, insulating a pipeline against wax) often changes the picture for another (that same insulation raises operating temperature, which lowers hydrate risk). Useful for framing why this whole area of research exists within a much bigger flow-assurance conversation. Once again, though:
nothing on bio-based candidates.
This goes deeper into how deposits actually build up along a pipe, using wall-growth and particle-transport models. What it adds for this project is confirmation that hydrate blockage isn't instantaneous; it's a progressive process, which is part of why a kinetic inhibitor only needs to buy time rather than stop formation outright to be useful. Its focus, though, is deposition modeling and gas-dominant systems specifically, with no inhibitor-performance data of the kind this study is trying to build context around.
A shorter mini-review of flow assurance problems generally is worth mentioning mainly for accessibility it's a good cross-check on terminology, useful when you want to be sure you're using "subcooling" or "flow assurance" the way the rest of the field does. It's brief by design, though, which means it doesn't engage deeply with hydrate inhibition or anything else specifically.

RESEARCH METHODOLOGY

3.1 Research Design

This study follows a laboratory-based, comparative experimental design rather than a field or simulation-based one. The central variable under investigation is solvent composition: three acetone-water ratios were used to extract material from the same coconut dust source, and the resulting extracts were then characterized side by side using identical analytical procedures, so that any differences observed in yield, functional-group, and thermal behaviour could be attributed to the solvent system rather than to inconsistencies in sample handling. This is, in effect, a controlled screening study; its purpose isn't to prove that coconut dust extract inhibits gas hydrates outright (that would require the flow-loop testing explicitly excluded from this project's scope), but to establish, systematically, which of three extraction conditions produces a candidate extract with the phytochemical and thermal profile the literature reviewed in Chapter Two associates with hydrate-inhibiting activity.

3.2 Materials

1. Coconut Coir Dust
2. Acetone
3. Handkerchief
4. Distilled Water
5. Thread
6. Vaseline

3.3 Apparatus and Equipment

The following equipment was used over the course of the extraction and characterization work:

1. Soxhlet Extraction Apparatus
2. Analytical weighing balance
3. Measuring cylinders
4. FTIR Spectrometer
5. A PerkinElmer thermogravimetric

6. Standard laboratory glassware
7. Stopwatch

3.4 Preparation of the Samples

Coconut coir dust was gathered and prepared before extraction by removing coarse debris, washing, drying, grinding, and sieving. A fixed mass of coconut dust was weighed and recorded for each of the three extraction runs before the material was loaded into the Soxhlet thimble. The three solvent systems, 100% acetone, 50/50 acetone-water, and 70/30 acetone-water, were each prepared by volume immediately before use, and 400 ml of the appropriate solvent mixture was measured out and charged into the Soxhlet apparatus for each run.



Figure 1: CCD (Residue)



Figure 2: CCD (Sieved)



Figure 3: Soxhlet extraction



Figure 4: CCD After Extraction

3.5 Experimental Workflow

The extraction procedure was carried out as follows for each of the three samples:

The weighed coconut dust sample was loaded into the Soxhlet thimble and placed into the extraction chamber.

400 ml of the appropriate solvent system was measured and added to the round-bottom flask.

The apparatus was assembled and heated to initiate the reflux-and-percolation cycle characteristic of Soxhlet extraction.

Extraction was allowed to continue until visual and procedural indicators suggested the process had run its course, with total extraction time recorded for each sample: 4 hours 30 minutes for OLCCDE 101, 4 hours 58 minutes for OLCCDE 102, and 4 hours 38 minutes for OLCCDE 103.

At the conclusion of each run, the coconut coir dust residue was reweighed to determine the mass lost to extraction, and the remaining solvent was measured to determine the volume recovered.

The resulting extract from each run was retained for characterization. Each of the three extracts was then analyzed separately by FTIR spectroscopy to identify the functional groups present, and by TGA/DTG to determine the thermal decomposition profile.

FTIR analysis was conducted on each sample under identical instrument settings (64 sample scans, 64 background scans, 16 cm^{-1} resolution, 4000–650 cm^{-1} range), and the resulting transmittance spectra and peak tables were recorded for each of the three samples.

TGA analysis was conducted on each sample under an identical heating program (30°C to approximately 920°C at 10°C/min), with sample masses of 11.200 mg (OLCCDE 101), 11.479 mg (OLCCDE 102), and 11.394 mg (OLCCDE 103), and both the weight-per cent-versus-temperature curve and its derivative (DTG) were recorded for each sample.

3.6 Data Analysis

Three forms of data were generated and analyzed in this study:

Extraction yield analysis: For each sample, the difference between the pre- and post-extraction weight of the coconut dust, alongside the volume of solvent recovered against the volume charged, was used as a simple indicator of how much material each solvent system was able to draw out of the coconut dust matrix, and how efficiently the solvent itself was recovered at the end of the process.

FTIR spectral analysis: The transmittance spectrum for each sample was examined for absorption bands in the regions associated with specific functional groups — broad O–H stretching (approximately 3200–3550 cm^{-1}) indicating hydroxyl-bearing phenolic compounds, C–H stretching (approximately 2850–2950 cm^{-1}) indicating aliphatic content, C=O stretching (approximately 1700–1750 cm^{-1}) indicating carbonyl-bearing compounds such as tannin's, and further fingerprint-region peaks below 1600 cm^{-1} indicating aromatic and other structural features — with the recorded peak tables cross-referenced against the reference band assignments established in the coconut coir literature reviewed in Chapter Two.

Thermal stability analysis: The TGA curve for each sample was examined for the number and temperature range of distinct mass-loss stages, and the DTG curve was used to identify the temperature of maximum decomposition rate for each stage, allowing the three samples' thermal profiles to be compared directly against one another and against the general lignocellulosic decomposition pattern established in Section 2.1.8.

3.7 Quality Control and Data Integrity

To maintain consistency across the three extraction runs, the same total solvent volume (400 mL) was used for each sample, and the same Soxhlet apparatus and general procedure were followed throughout, so that any differences observed between samples could be attributed to solvent composition rather than to procedural variation. FTIR and TGA analyses for all three samples were conducted under identical instrument settings and heating programs, ensuring that spectral and thermal comparisons between samples were made on a like-for-like basis rather than being confounded by differing analytical conditions. All raw instrument outputs — FTIR peak tables and TGA/DTG data files — were retained in full alongside the processed results presented in Chapter Four, so that the analysis could be independently verified or reprocessed if required.

RESULTS AND DISCUSSION

4.1 Data Presentation

Three coconut coir dust extracts were produced and characterized in this study, each named for the solvent system used to obtain it. Before getting into what each result means, it's worth laying out exactly what was measured, since the discussion that follows leans on comparing all three side by side.

Table 1: Extraction Result Data

SAMPLE	SOLVENT SYSTEM	CCD WEIGHT BEFORE	CCD WEIGHT AFTER	SOLVENT USED	SOLVENT RECOVERED	EXTRACTION TIME
OLCCDE101	100% Acetone	63.2 g	62.5 g	400 ml	210 ml	4 hrs 30mins
OLCCDE102	50% Acetone & 50% water	69.2 g	67.7 g	400 ml	180 ml	4 hrs 58 mins
OLCCDE103	70% Acetone & 30% water	64.7 g	63.9 g	400 l	140 ml	4 hrs 38 mins

Table 2: Extraction Yield Data

SAMPLE	SOLVENT SYSTEM	CCD BEFORE	CCD AFTER	MASS LOST	EXTRAC TION YIELD	SOLVENT RECOVERED	TIME TAKEN
OLCCDE101	100% ACETONE	63.2 g	62.5 g	0.7 g	1.107%	210/400 mL (52.5%)	4 hrs 30mins
OLCCDE102	50% Acetone/50% Water	69.2 g	67.7 g	1.3 g	2.167 %	180/400 mL (45%)	4 hrs 58mins

OLCCDE103	70% Acetone/30%	64.7 g	63.9 g	0.8 g	1.236%	140/400Ml (35%)	4 hrs 38 mins
	Water						

4.2 Extraction Yield and Efficiency

By weight loss alone, the 50/50 acetone-water blend (OLCCDE 102) pulled the most material out of the coconut coir dust 2.17%, nearly double the yield from pure acetone (OLCCDE 101, 1.11%) and noticeably ahead of the 70/30 blend (OLCCDE 103, 1.24%). That's a genuinely interesting result, and it's worth being upfront that it doesn't line up neatly with Israel et al. (2011), who found the 70/30 acetone-water ratio gave the best extraction performance on the same source material. A few things could explain the difference: a different batch or maturity of coconut dust, a different definition of "extraction performance" (Israel et al. weighted their assessment toward phytochemical screening results rather than raw mass loss alone), or simply natural variation between extraction runs. Rather than force a match with the literature, it's more honest to treat this as a genuine point of divergence worth flagging for anyone following up on this work with a larger sample size or repeated trials.

Solvent recovery said a clearer, more consistent story: recovery dropped steadily as the water content of the solvent rose, from 52.5% for pure acetone down to 35% for the 70/30 blend. This is a reasonably intuitive finding acetone is far more volatile than water, and a solvent system carrying more water will simply retain more liquid within the moist, fibrous coconut dust matrix (and lose more to evaporation losses that don't return through the Soxhlet condenser as cleanly), rather than anything specific to how much extract was being pulled out.

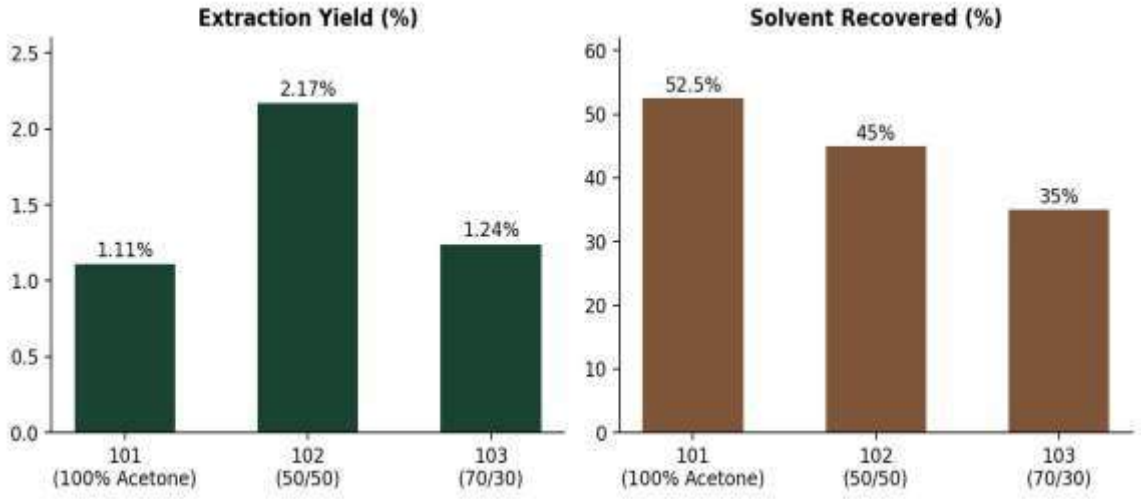


Figure 5: Extraction Yield and Efficiency

4.3 FTIR Spectral Analysis and Functional Group Identification

The three spectra tell a fairly coherent chemical story once they're read side by side, and the clearest signal in the whole data-set is what happened to the O–H stretching region.

The broad hydroxyl absorption band, the fingerprint of phenolic and tannin-type compounds, showed up at 77.50% transmittance for OLCCDE 101 (100% acetone), dropped to 51.63% for OLCCDE 102 (50/50), and dropped further still to 43.75% for OLCCDE 103 (70/30). Lower transmittance at this band means deeper absorption, which means more hydroxyl-bearing material is present. Read plainly: the more water was added to the solvent, the more hydroxyl-rich compound the extraction pulled out. That's exactly the pattern predicted by the polarity argument laid out in Chapter Two — water is a strongly polar solvent, and polyphenols and tannin's, being polar and hydrogenbond-rich themselves, dissolve into a more aqueous system far more readily than into pure acetone. This is arguably the single most useful finding in the entire characterization exercise, because hydroxyl-bearing phenolics are precisely the compound class the corrosion-inhibition literature and the hydrophobic-amino-acid KHI study both associate with the kind of hydrogen-bond interaction that plausibly matters to hydrate inhibition.

The number of resolved peaks tells a second, related story. OLCCDE 101 produced a rich, ten-peak spectrum spanning the full fingerprint region (1103–1714 cm^{-1}) in addition to its C–H and O–H bands, suggesting a chemically diverse extract — likely dominated by less polar constituents such as waxes, lipids, and aliphatic esters that dissolve well in pure acetone but leave a lot of distinct, well-separated functional-group signatures. OLCCDE 102 and 103, by contrast, produced noticeably sparser spectra (four and five peaks respectively), each dominated by that same deep, broad O–H band. This is consistent with a simpler picture: as water content rises, extraction becomes increasingly selective for one or two dominant compound classes hydroxyl-rich phenolics chief among them rather than pulling out the wider chemical mixture that pure acetone manages to dissolve.

Both OLCCDE 102 and 103 also showed a peak in the 2094–2117 cm^{-1} region, which is worth flagging honestly rather than glossing over. This region doesn't correspond to any of the functional groups this study set out to screen for — it sits in a range more commonly associated with C≡C or C≡N stretching, or occasionally with instrumental artefacts from atmospheric interference. Neither explanation can be confirmed from FTIR data alone, and this is a fair example of exactly the limitation flagged in Chapter Two: FTIR identifies functional-group classes reliably, but resolving an ambiguous peak like this one would require a complementary technique such as GC-MS. It's noted here rather than left out, but it shouldn't be over-interpreted.

The peak near 1632 cm^{-1}, present in both OLCCDE 102 and 103, is more straightforward to interpret — it falls squarely in the range associated with aromatic C=C ring stretching, consistent with the flavonoid and tannin content Israel et al. (2011) confirmed in comparably extracted coconut coir dust. OLCCDE 101's carbonyl peak at 1714.6 cm^{-1}, meanwhile, sits in the range typical of ester or carboxylic acid C=O stretching — plausible given that pure acetone would be expected to draw out more lipid and wax-type material than the water-containing blends. expected to draw out more lipid and wax-type material than the water-containing blends.

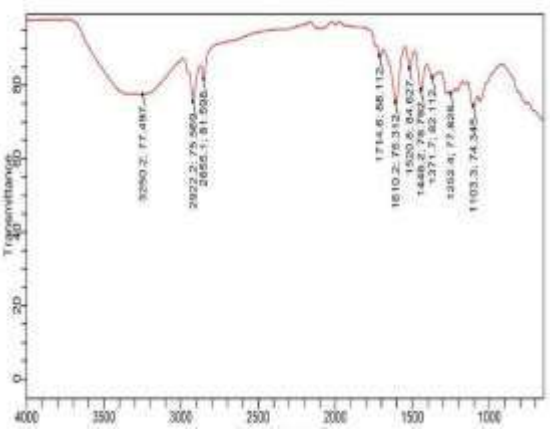


Figure 6: FTIR spectrum of OLCCDE 101 (100% acetone)

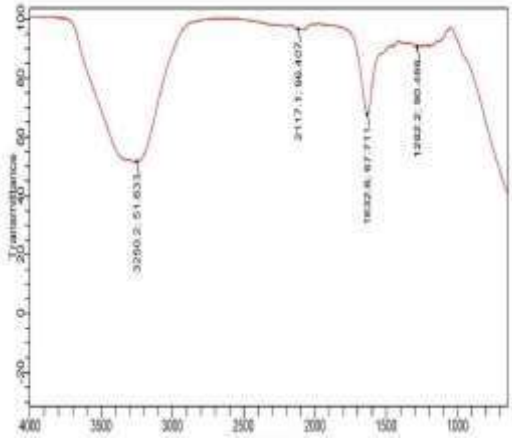


Figure 7: FTIR spectrum of OLCCDE 102 (50/50 acetone-water)

Ten distinct peaks are resolved across the fingerprint region, consistent with a chemically diverse extract dominated by less polar material.

A markedly deeper O–H band appears near 3250 cm^{-1}, alongside fewer, broader peaks than OLCCDE 101.

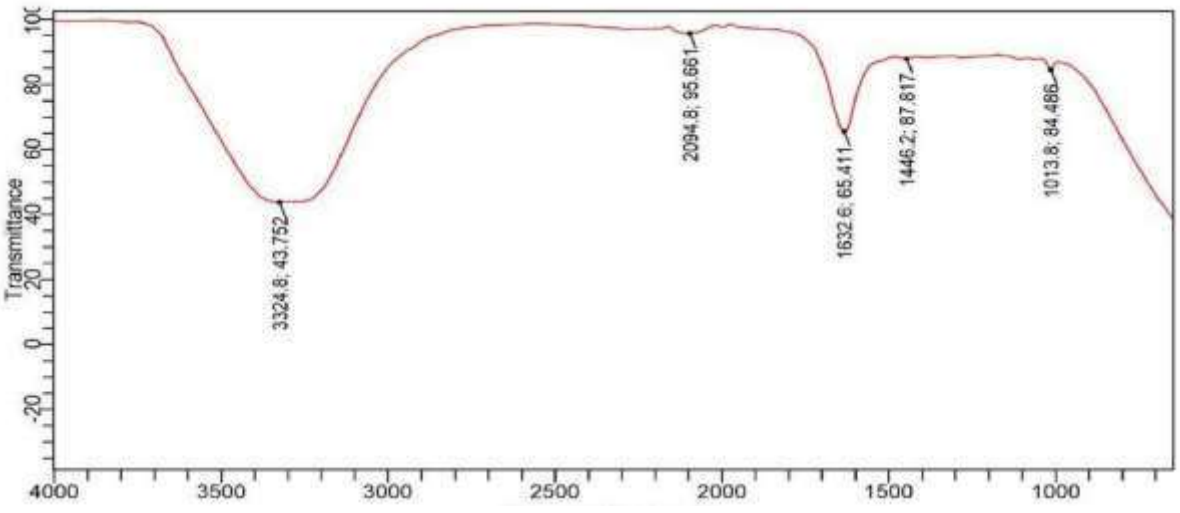


Figure 8: FTIR spectrum of OLCCDE 103 (70/30 acetone-water). This sample shows the deepest O–H absorption of all three, along with the aromatic C=C peak near 1632 cm^{-1} associated with flavonoids and tannins.

4.4 Thermogravimetric (TGA/DTG) Analysis

All three samples followed the same broad three-stage decomposition pattern described in Chapter Two for lignocellulosic material: a small early mass loss attributable to residual moisture, a dominant decomposition event in the low-to-mid 200s through high 300s °C range, and a long, slow tail toward a stable char residue by around 900°C. Where the three samples differ is in the details of that pattern, and those details are informative.

OLCCDE 101 left the largest residue at the end of the heating program — roughly 12%, against roughly 9.5% for OLCCDE 102 and 9–9.3% for OLCCDE 103. A higher final residue means, in effect, less of the sample's total mass was volatilized or thermally decomposed over the course of the run. Combined with the FTIR picture, this fits together sensibly: OLCCDE 101's more chemically diverse, less hydroxyl-dominated extract appears to contain a larger proportion of thermally robust material, while the more phenolic- and tannin-rich extracts (102 and 103) decomposed more completely, consistent with polyphenolic compounds generally being less thermally stable at high temperature than waxes or more structurally rigid aliphatic material.

The DTG curves sharpen this picture further. OLCCDE 101 showed its sharpest rate of mass loss around 290–300°C, at a peak rate of roughly −4.6% per minute, with a small secondary shoulder in the 70–150°C range reflecting minor volatile or moisture loss ahead of the main decomposition event. OLCCDE 102 showed a broader, somewhat gentler main decomposition peak at a similar temperature (around 290–300°C) but a noticeably lower peak rate, roughly 3.65% per minute a slower, more gradual breakdown than either of the other two samples. OLCCDE 103 showed the sharpest and most intense decomposition of the three, peaking slightly earlier, around 270–290°C, at a rate approaching 4.5 to 4.7% per minute, and distinctively a clear, well-defined secondary shoulder around 90–100°C, more pronounced than the equivalent feature in OLCCDE 101 and essentially absent in OLCCDE 102. That secondary low-temperature shoulder in OLCCDE 103 is worth a moment's attention, since it's the clearest visual difference between the three DTG curves. It most plausibly reflects loss of more tightly bound moisture or a low-boiling volatile fraction specific to the 70/30 acetone-water extract's composition, though pinning down exactly which compound is responsible would again require a complementary analytical technique beyond the scope of this study's FTIR and TGA characterization.

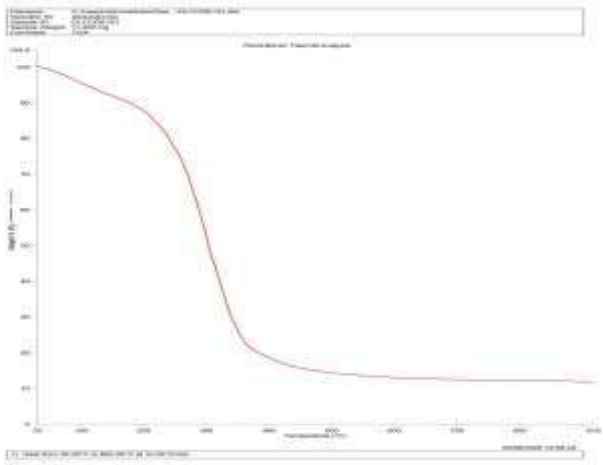


Figure 9:TGA curve for OLCCDE 101 (100% Acetone)

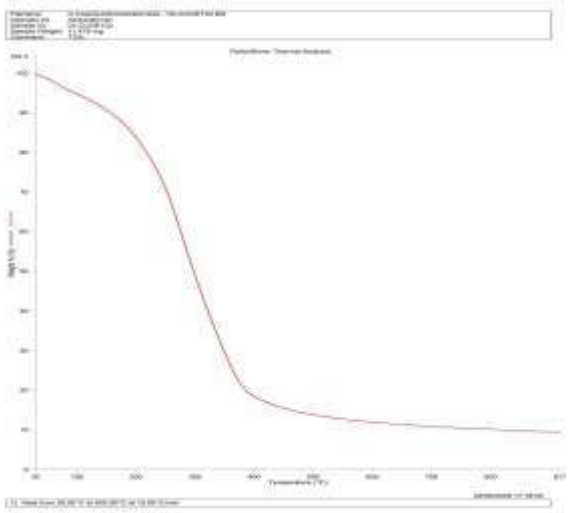


Figure 10: TGA curve for OLCCDE 102 (50/50% Acetone-Water)

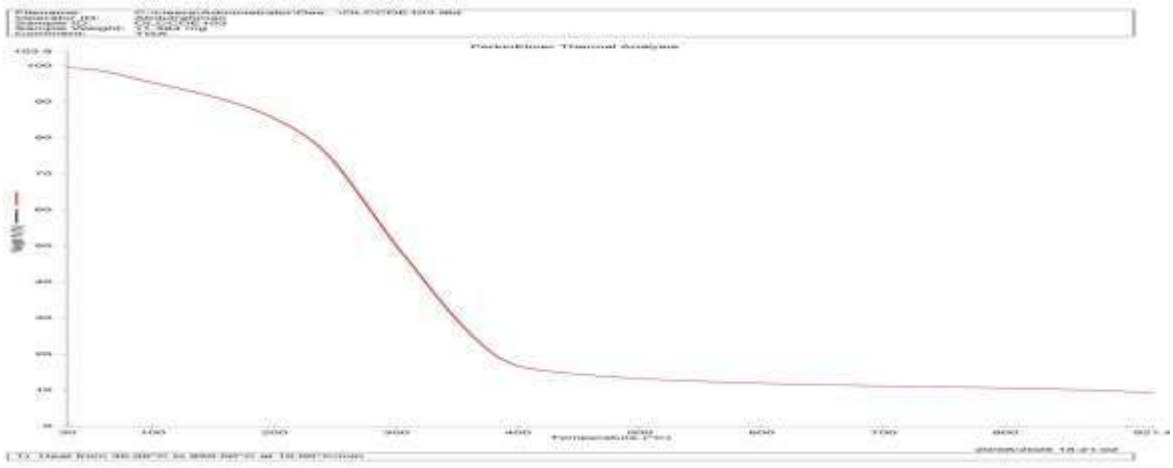


Figure 11: TGA curve for OLCCDE 103 (70/30 acetone-water).

OLCCDE 101 left the largest residue at the end of the run, roughly 12%, against roughly 9.5% for OLCCDE 102 and 9 to 9.3% for OLCCDE 103. A higher final residue means less of the sample’s total mass was volatilized or decomposed. Combined with the FTIR picture, this makes sense: OLCCDE 101’s more diverse, less hydroxyldominated extract seems to contain more thermally robust material, while the more phenolic- and tannin-rich extracts decomposed more completely, which fits with polyphenolic compounds generally being less thermally stable at high temperature than waxes or structurally rigid aliphatic material.

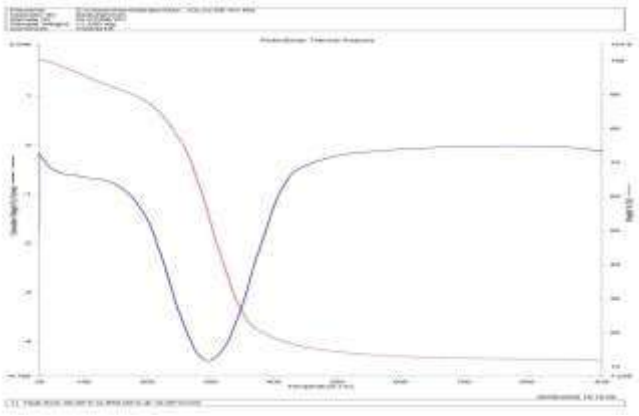


Figure 12: DTG curve for OLCCDE 101,

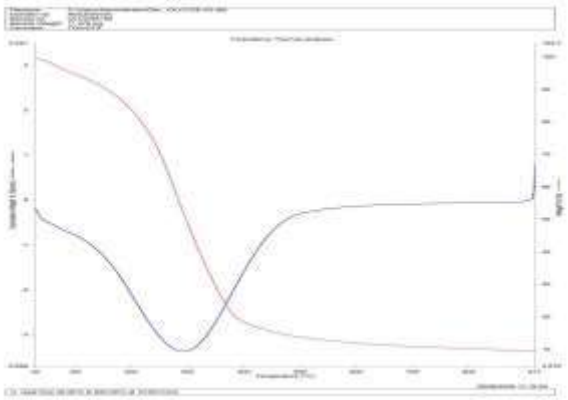


Figure 13: DTG curve for OLCCDE 102

Figure 12 is showing peak decomposition rate of roughly 4.6%/min near 290–300°C, plus a small shoulder in the 70–150°C range. Figure 13 is showing the gentlest, broadest main decomposition peak of the three samples, at roughly 3.65%/min.

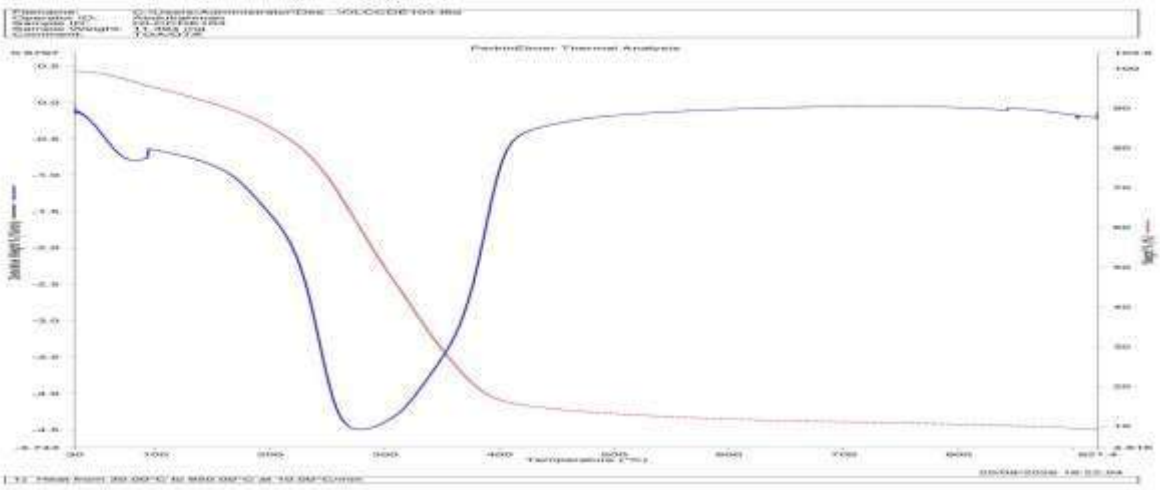


Figure 14: DTG curve for OLCCDE 103

This is showing the sharpest decomposition of the three (approximately 4.5 to 4.7%/min, peaking near 270–290°C) along with a distinct low-temperature shoulder around 90–100°C.

4.5 Comparative Discussion Across Solvent Systems

Pulling the three analyses together, a reasonably coherent picture of each extract emerges:

OLCCDE 101 (100% acetone): produced a low-yield, chemically diverse extract, rich in fingerprint-region functional groups but comparatively weak in hydroxyl content, and the most thermally robust of the three, leaving the largest final char residue.

OLCCDE 102 (50/50 acetone-water): produced the highest extraction yield by weight, a strongly hydroxyldominated FTIR signature, and the most gradual, lowest-intensity thermal decomposition of the three — an extract that comes out in the largest quantity but breaks down the least abruptly under heat.

OLCCDE 103 (70/30 acetone-water): produced a moderate yield, the strongest hydroxyl absorption of all three samples (suggesting the highest relative phenolic/tannin content), and the sharpest, most intense thermal decomposition, alongside a distinct low-temperature volatile shoulder not clearly present in OLCCDE 102. None of the three samples stands out as an unambiguous "winner" across every metric simultaneously, and it would be overreaching to declare one outright best without the flow-loop performance data this study's scope deliberately excludes (Section 1.4). What can be said, on the evidence gathered here, is that OLCCDE 103 shows the strongest phytochemical signal of the compound class hydroxyl-rich phenolics and tannins — that the literature reviewed in Chapter Two most consistently associates with hydrate-inhibiting activity in comparable plant and coconut-derived extracts, while OLCCDE 102 offers the practical advantage of the highest extraction yield. Both would be reasonable candidates to carry forward into future flow-loop testing; OLCCDE 101, while thermally the most robust, shows the weakest hydroxyl signature of the three and would appear the least promising candidate on the phytochemical evidence alone.

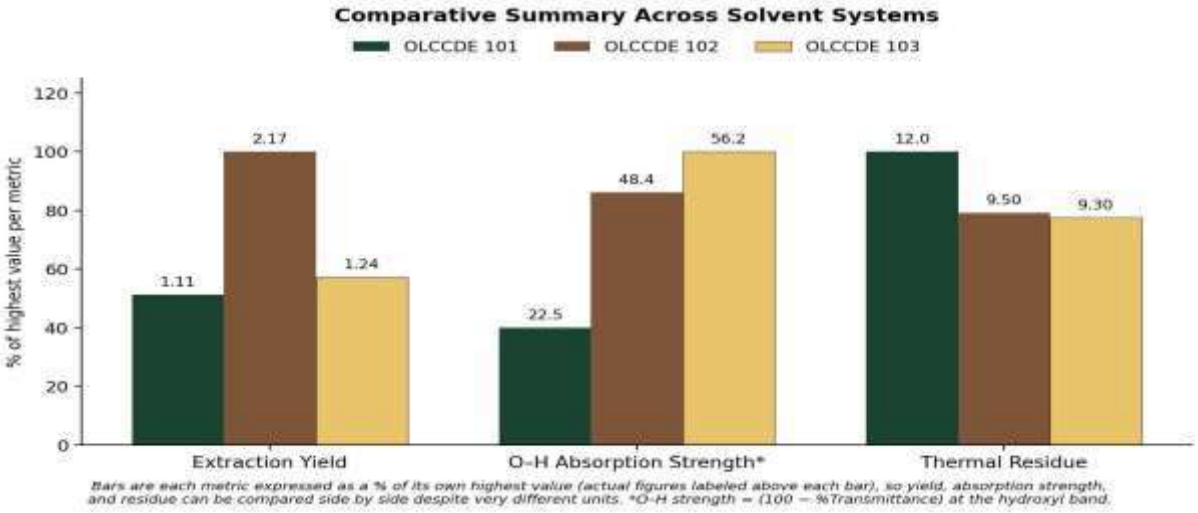


Figure 15: Extraction yield, hydroxyl (O–H) absorption depth, and TGA final residue for all three samples, each metric scaled to its own maximum so the three very different units can be compared side by side on one chart.

OLCCDE 102 leads on yield, OLCCDE 103 leads on hydroxyl content, and OLCCDE 101 leads on thermal residue.

4.6 Discussion in Relation to Existing Literature

The pattern of increasing hydroxyl content with increasing solvent polarity observed here lines up with the general extraction-methodology literature discussed in Section 2.2.7, which identifies solvent polarity as the single most important variable governing which compound classes come out of a plant or biomass matrix. It's also broadly consistent with Israel et al.'s (2011) confirmation of tannin and flavonoid content in acetone-water extracts of coconut coir dust, even though this study's specific yield ranking did not replicate their reported optimum ratio.

The tannin- and phenolic-associated FTIR bands identified in OLCCDE 102 and 103 are the same compound classes that Ndoma-egba et al. (2025) confirmed present in the Moringa oleifera extract that achieved 60% hydrate inhibition efficiency, and the same classes the plant-based corrosion-inhibitor review (Section 2.2.7) associates with surface-adsorbing, interface-active behaviour. Taken together with the hydrogen-bonding mechanism proposed in the hydrophobic amino acid KHI study (Section 2.2.3): where lower hydrophobicity correlated with stronger inhibition, the hydroxyl-rich chemistry confirmed here in OLCCDE 102 and 103 is at least consistent with the kind of chemistry that literature associates with hydrate-inhibiting potential. This is circumstantial support rather than direct proof, and it should be stated no more strongly than that: nothing in this study's scope demonstrates that CCDE actually inhibits hydrate formation, only that its chemistry is not inconsistent with compounds that have been shown to do so elsewhere.

On the thermal side, the finding that extraction solvent shaped thermal decomposition behaviour as much as it shaped functional-group content echoes the coconut coir pith lignin study discussed in Section 2.2.6, which found that different extraction protocols produced lignin with meaningfully different thermal stability. All three CCDE samples, regardless of solvent system, comfortably survive the modest temperature range (well under 100°C) that a pipeline inhibitor would realistically encounter in service, so thermal stability does not appear to be a limiting concern for any of the three candidates at this stage.

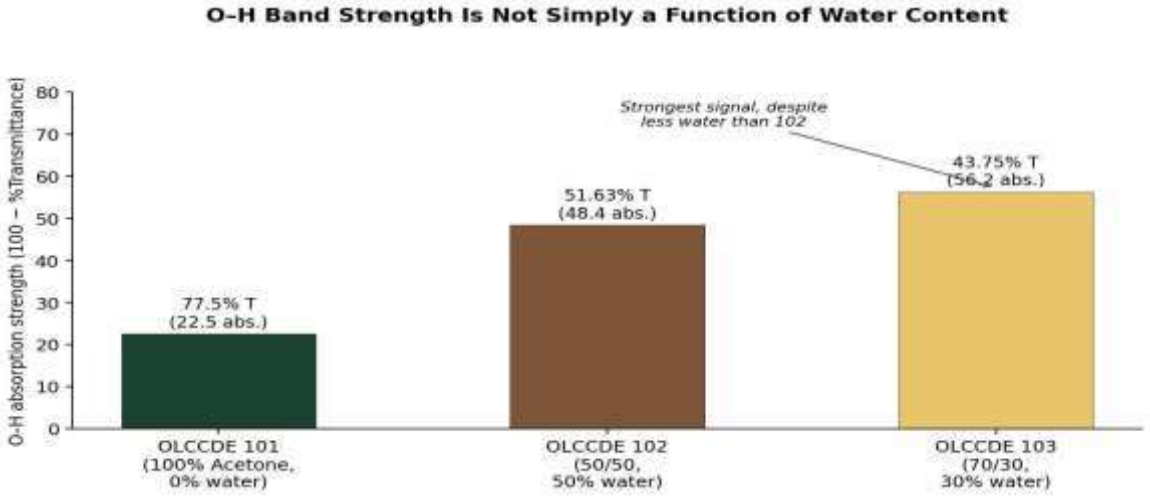


Figure 16: O–H band transmittance across the three solvent systems,

In the order tested. OLCCDE 103 (70/30 acetone-water) gives the strongest hydroxyl signal of the three, despite carrying less water than OLCCDE 102

5.1 Conclusion

This study asked whether coconut coir dust, a material treated until now as little more than agricultural waste, might carry the chemical fingerprints tied to effective, environmentally friendly gas hydrate inhibition. The answer, on the evidence gathered here, is a cautious but genuine yes. Extracted with the right solvent system, coconut dust yields a hydroxyl- and phenolic-rich material chemically consistent with the compound classes already shown, across a growing body of Nigerian flow-loop research, to rival methanol's hydrate-suppressing performance at a fraction of the dosage. It survives realistic pipeline temperatures without difficulty, and it comes from a feedstock that's abundant, cheap, and currently near-worthless.

This study was always meant as a first step rather than a final word, though. It characterises; it doesn't test. What it offers is a clear characterisation baseline: three solvent systems compared, ranked, and chemically profiled, laying groundwork for the flow-loop testing that would actually confirm hydrate-inhibiting performance rather than infer it. If that next step bears out what this study's data suggests, coconut coir dust extract would join a small but growing list of agricultural waste products that turn out to have real value the industry hasn't noticed yet- the kind of unglamorous, practical finding that flow assurance research is often built on.

REFERENCES

1. Almashwali, A. A., Bavoh, C. B., Lal, B., Khor, S. F., Jin, Q. C., & Zaini, D. (2022). Gas hydrate in oil-dominant systems: A review. *ACS Omega*, *7*(31),27021–27037. https://doi.org/10.1021/acsomega.2c02278
2. Asikoko, F., Okologume, W. C., Appah, D., & Aimikhe, V. (2024). Experimental investigation of cassava (*Manihot esculenta*) leaf extract as a green inhibitor of gas hydrate formation. *Biomass Conversion and Biorefinery*, *14*(16), 19383–19392. https://doi.org/10.1007/s13399-023-04213w
3. Asoka Panamgama, L., & Peramune, P. R. U. S. K. (2018). Coconut coir pith lignin: A physicochemical and thermal characterization. *International Journal of Biological Macromolecules*, *113*, 1149–1157. https://doi.org/10.1016/j.ijbiomac.2018.03.012
4. Elechi, V. U., Ikiensikimama, S. S., Ajienka, J. A., Akaranta, O., Onyekonwu, M. O., Odutola, T. O., & Okon, E. O. (2018). *Gas hydrate inhibition in a simulated offshore environment using local inhibitor* (SPE-193439-MS). SPE Nigeria Annual International Conference and Exhibition, Lagos, Nigeria. https://doi.org/10.2118/193439-MS
5. Englezos, P. (1993). Clathrate hydrates. *Industrial & Engineering Chemistry Research*, *32*(7),1251–1274. https://doi.org/10.1021/ie00019a001
6. Englezos, P. (2026). Clathrate hydrate crystallization. *The Canadian Journal of Chemical Engineering.* https://doi.org/10.1002/cjce.70411
7. Israel, A. U., Ogali, R. E., Akaranta, O., & Obot, I. B. (2011). Extraction and characterization of coconut (*Cocos nucifera* L.) coir dust. *Songklanakarin Journal of Science and Technology*, *33*(6), 717–724. *(No DOI assigned by publisher.)*
8. Kakwaya, J., Madirisha, M., Kilulya, K., & Lugwisha, E. (2023). Isolation and performance test of green low dosage hydrate inhibitors from local materials for improving flow assurance in oil and gas industry. *Tanzania Journal of Engineering and Technology*, *42*(2),95–112. https://doi.org/10.52339/tjet.v42i2.806
9. Kelland, M. A., Dirdal, E. G., & Knutsen, C. M. (2024). Comparing the kinetic hydrate inhibition performance of linear versus branched polymers. *ACS Omega*, *9*(11),12956–12966. https://doi.org/10.1021/acsomega.3c09260
10. Khan, M. N., Warrier, P., & Koh, C. A. (2024). An overview of thermodynamics and growth kinetics of gas hydrate systems. *Transactions of the Indian Institute of Metals*, *77*, 4467–4479. https://doi.org/10.1007/s12666-023-03095-w
11. Kumar, A. (2023). Perspectives of flow assurance problems in oil and gas production: A mini-review. *Energy & Fuels*, *37*(12), 8142–8159. https://doi.org/10.1021/acs.energyfuels.3c00843
12. Liao, D., Su, G., Liang, L., He, J., Ye, H., Xiao, Q., Xiong, Y., Wang, D., Liu, L., & Luo, X. (2024). Preparation **and** application of an economical and environmentally friendly hydrate inhibitor in gas field development. *PLOS ONE*, *19*(7), e0307109. https://doi.org/10.1371/journal.pone.0307109
13. Ndoma-egba, S., Uduefe, E. S., & Okuma, S. O. (2025). Experimental assessment of Moringa oleifera as an environmentally friendly inhibitor solution for gas hydrate control. *Journal of Materials Engineering, Structures and Computation*, *4*(2), 19–30. https://doi.org/10.5281/zenodo.15576356
14. Odutola, T. O., Ajienka, J. A., Onyekonwu, M. O., & Ikiensikimama, S. S. (2017). Design, fabrication and validation of a laboratory flow loop for hydrate studies. *American Journal of Chemical Engineering*, *5*(3-1), 28–41. https://doi.org/10.11648/j.ajche.s.2017050301.14
15. Odutola, T. O., & Ugwu, C. E. (2019). Simulation of laboratory hydrate loop using Aspen Hysys. *Engineering and Applied Sciences*, *4*(3), 52–58. https://doi.org/10.11648/j.eas.20190403.11

16. Okon, O. E., Ikiensikimama, S. S., Wachikwu-Elechi, V. U., Ajienka, J. A., & Akaranta, O. E. (2023). Gas hydrate inhibition: Performance of an agro-waste based locally formulated inhibitor. *Journal of Dispersion Science and Technology, 44*(12), 2330–2339. https://doi.org/10.1080/01932691.2022.2074858
17. Rahmanian, N., Söyler, N., Wande, F. M., & Hashemi, H. (2025). An investigation on hydrate prediction and inhibition: An industrial case study. *The Canadian Journal of Chemical Engineering*, *103*(1), 396–409. https://doi.org/10.1002/cjce.25357
18. Sa, J.-H., Kwak, G.-H., Lee, B. R., Park, D.-H., Han, K., & Lee, K.-H. (2013). Hydrophobic amino acids as a new class of kinetic inhibitors for gas hydrate formation. *Scientific Reports, 3*, 2428. https://doi.org/10.1038/srep02428
19. Sabore, K. J., Thuo, G. J., Igadwa, M. J., & Joyline, G. (2024). Comparative analysis of coir fibers from mature and immature coconut husk waste from Kenyan coastal region. *Journal of Natural Fibers, 21*, 2390078. https://doi.org/10.1080/15440478.2024.2390078
20. Tang, C., Farhadian, A., Berisha, A., Deyab, M. A., & Liang, D. (2023). Novel biosurfactants for effective inhibition of gas hydrate agglomeration and corrosion in offshore oil and gas pipelines. ACS Sustainable Chemistry & Engineering 11(1), 353–367. https://doi.org/10.1021/acssuschemeng.2c05716
21. Thakre, N., & Jana, A. K. (2021). Physical and molecular insights to clathrate hydrate thermodynamics. *Renewable and Sustainable Energy Reviews, 135*, 110150. https://doi.org/10.1016/j.rser.2020.110150
22. Xin, Z., Jiang, Z., Wang, F., & Zhang, Y. (2025). Review on flow assurance issues in natural gas pipeline transmission systems and solutions to hydrate deposition. *Chemical Engineering Science, 306*, 121290. https://doi.org/10.1016/j.ces.2025.121290
23. Zhang, S.-W., Shang, L.-Y., Zhou, L., & Lv, Z.-B. (2022). Hydrate deposition model and flow assurance technology in gas-dominant pipeline transportation systems: A review. *Energy & Fuels*, *36*(4), 1747–1775 https://doi.org/10.1021/acs.energyfuels.1c03812